Flow Characteristics in Spin-Up of a Three-Layer Fluid

Evgeny Sviridov, Jae Min Hyun*

Department of Mechanical Engineering, Korea Advanced Institute of Science and Technology, 373-1 Kusong-dong, Yusong-gu, Daejeon 305-701, Korea

A numerical study is made of the spin-up from rest of a three-layer fluid in a closed, vertically-mounted cylinder. The densities in the upper layer ρ_1, middle layer ρ_2 and lower layer ρ_3 are $\rho_3>\rho_2>\rho_1$, and the kinematic viscosities are left arbitrary. The representative system Ekman number is small. Numerical solutions are obtained to the time-dependent axisymmetric Navier-Stokes equations, and the treatment of the interfaces is modeled by use of the Height of Liquid method. Complete three-component velocity fields, together with the evolution of the interface deformations, are depicted. At small times, when the kinematic viscosity in the upper layer is smaller than in the middle layer, the top interface rises (sinks) in the central axis (peripheral) region. When the kinematic viscosity in the lower layer is smaller than in the middle layer, the bottom interface rises (sinks) in the periphery (axis) region. Detailed shapes of interfaces are illustrated for several cases of exemplary viscosity ratios.

Key Words : Rotaing Flow, Spin-Up, Inhomogeneous Fluid

Nomenclature

A : Aspect ratio, R/H [−]

Fr : Froude number, $\frac{(\Omega R)^2}{gH}$ [−]

g : Gravity [m/s^2]

E : Ekman number, $\nu/\Omega_f R^2$ [−]

H : Height of cylinder [m]

h_0 : The original height at the initial state [m]

R : Radius of cylinder [m]

Re : Reynolds number, $\Omega_f R^2/\nu$ [−]

p : Dimensionless pressure [−]

u^* : Reference velocity, ΩR [m/s]

t : Time [s]

(V_r, V_φ, V_z) : Dimensionless velocity components corresponding to (r, ϕ, z)

(r, ϕ, z) : Dimensionless (radial, azimuthal, vertical) coordinates in cylindrical system

Greek symbols

(α, β, γ) : Indicators [−]

Ω : Rotation rate [s^{-1}]

ν : Kinematic viscosity [m^2/s]

ν_1, ν_2 : Kinematic viscosity ratios, $\nu_1=\nu_1^*/\nu_3^*$, $\nu_2=\nu_2^*/\nu_3^*$ [−]

ρ : Dimensionless density, ρ^*/ρ_3 [−]

ρ_1, ρ_2 : Density ratios, $\rho_1=\rho_1^*/\rho_3^*$, $\rho_2=\rho_2^*/\rho_3^*$ [−]

τ : Dimensionless time, $t\Omega$ [−]

ψ : Dimensionless meridional stream function [−]

Subscripts

1 : Values in upper layer

2 : Values in middle layer

3 : Values in lower layer

f : Final state

i : Initial state

Superscripts

$*$: Dimension values

* Corresponding Author,
E-mail : jmhyun@kaist.ac.kr
TEL : +82-42-869-3012; **FAX** : +82-42-869-3210
Department of Mechanical Engineering, Korea Advanced Institute of Science and Technology, 373-1 Kusong-dong, Yusong-gu, Daejeon 305-701, Korea.
(Manuscript **Received** July 21, 2005; **Revised** December 27, 2005)

1. Introduction

Consider an incompressible viscous fluid (den-

sity ρ, kinematic viscosity ν) which completely fills a vertically-mounted, closed cylindrical container (radius R, height H, and the aspect ratio $A=H/R\sim O(1)$). At the initial state, both the fluid and the cylindrical container rotate steadily about the central longitudinal axis at rotation rate Ω_i. At time $t=0$, the rotation rate of the cylinder is impulsively increased to $\Omega_f(=\Omega_i+\Delta\Omega)$. In response to this change, the fluid undergoes an adjustment process involving a transient three-component velocity field. This overall time-dependent flow process is termed the spin-up, and the problem has occupied the center stage in basic rotating flow research as well as in technological applications. As is in engineering situations, attention is focused to the cases when the representative Reynolds number ($Re\equiv\Omega_f R^2/\nu$) is large so that a boundary layer-type global flow prevails. In the studies of rotating flow, the Ekman number, $E\equiv\nu/\Omega_f R^2$, is also widely used. In industrial applications, knowledge of spin-up flows is relevant to the design and operation of rotating fluid machinery, chemical mixers and material processing devices, to name a few.

For the linearized spin-up from an initial state of rigid-body rotation, i.e., $\Omega_i\neq 0$, $\Delta\Omega/\Omega_f\ll 1$, the classical treatise of Greenspan & Howard (1963) established that the entire process involves three stages: first, the boundary layer forms on the endwall disks over $O(\Omega_f^{-1})$; second, the bulk of the fluid is substantially spun-up over the spin-up time scale $O(\mathbf{Re}^{1/2}\ \Omega_f^{-1})$; third, the remaining small disturbances are adjusted over the diffusion time scale $O(Re\Omega_f^{-1})$.

The main mechanism for spin-up is the inducement of meridional flow in the interior by boundary layer suction. In the inviscid interior, the radially-inward moving fluid, which maintains the angular momentum conservation, causes the increase of angular velocity at a given radial location. It is, therefore, important to point out that the global spin-up is accomplished over the spin-up time scale, which is an order-of-magnitude smaller than the diffusion time scale.

The nonlinear spin-up from rest ($\Omega_i=0$, $\Delta\Omega/\Omega_f=1$) poses challenging fundamental issues. The basic model due to Wedemeyer (1964) clearly demonstrated that the principal dynamic element remains to be the meridional circulation in the interior, which is induced by the boundary layers on the endwall disks. In this case, however, the interior at the initial state was at rest. One significant feature is the presence of the radially-inward propagating velocity shear front, which separates the non-rotating and rotating regions. These global flow features are captured by the original model of Wedemeyer (1964), which was later extended by Weidman (1976) and others.

The above-stated studies deal with the case when the fluid is homogeneous and of constant density. The spin-up from rest of two immiscible fluids of different densities and kinematic viscosities in a cylinder was investigated theoretically by several authors, e.g., Baker & Israeli (1981). Lim et al. (1993) and Kim & Hyun (1994) modified the Wedemeyer model to describe the spin-up from rest of a two-layer liquid system. These results were in reasonable agreement with the laboratory observations. In these models, the density of the lower-layer ρ_1 is greater than that of the upper layer ρ_u, but the values of kinematic viscosities of the two layers are left arbitrary. Of particular interest here is the evolution of the initially-flat interface between the two layers. The final-state shape of the interface is a paraboloid; however, the transient pattern of the interface during spin-up needs a careful scrutiny. It was pointed out in Lim et al. (1993) that, if the kinematic viscosity of the upper layer ν_u is greater than that of the lower layer ν_1, the upper layer spins up faster. Therefore, in this case, at small times after the abrupt start of the rotation of the cylinder, the interface bulges upward at small radii near the axis and sinks downward at large radii near the sidewall. These features are peculiar to the nonlinear spin-up process of a two-layer fluid system.

The purpose of the present study is to extend the prior models to depict spin-up from rest of a three-layer fluid. These efforts will shed light to the transient process of adjustment to the impulsively-started rotating container of a multi-layered fluid system. The time-dependent behavior of the interfaces, which separate the layers of fluid

of different densities and viscosities, will be illustrated. In this paper, numerical solutions are acquired to the governing Navier-Stokes equations. The numerical data will be processed to render portrayals of the interfaces and the three-component velocity fields in the cylinder.

2. Formulation of the Problem

The cylinder is filled with three equal-volume layers of immiscible fluids, as shown in Fig. 1. At the initial state of rest, the horizontal interfaces are located at height $h_3=H/3$ and $h_2=2/3H$ above the bottom endwall disk. The densities of the lower, middle and upper layer are respectively ρ_3^*, ρ_2^* and ρ_1^*, $\rho_3^*>\rho_2^*>\rho_1^*$. As remarked earlier, the values of kinematic viscosities of the three layers are left arbitrary. At the initial instant $t=0$, the cylinder is abruptly set into rotation Ω about its symmetry axis z^*, and the task is to describe the ensuing time-dependent motions of fluids.

The governing time-dependent axisymmetric Navier-Stokes equations, in dimensionless form, are:

$$\frac{1}{r}\frac{\partial(rV_r)}{\partial r}+\frac{\partial V_z}{\partial z}=0 \tag{1}$$

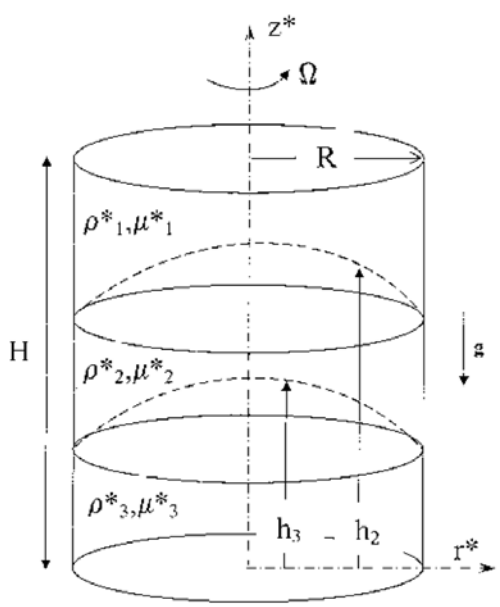

Fig. 1 Schema of flow configuration

$$\frac{1}{A}\frac{\partial(\rho V_r)}{\partial\tau}+\frac{1}{r}\frac{\partial}{\partial r}(\rho r V_r V_r)+\frac{\partial}{\partial z}(\rho V_z V_r)-\rho\frac{V_\varphi^2}{r}$$
$$=-\frac{\partial p}{\partial r}+E_3\left(\frac{1}{r}\frac{\partial}{\partial r}\left(2\mu r\frac{\partial V_r}{\partial r}\right)+\frac{\partial}{\partial z}\left(\left(\frac{\partial V_r}{\partial z}+\frac{\partial V_z}{\partial r}\right)\right)-2\mu\frac{V_r}{r^2}\right) \tag{2}$$

$$\frac{1}{A}\frac{\partial(\partial V\varphi)}{\partial\tau}+\frac{1}{r}\frac{\partial}{\partial r}(\rho r V_r V_\varphi)+\frac{\partial}{\partial z}(\rho V_z V_\varphi)+\rho\frac{V_\varphi V_r}{r}$$
$$=E_3\left(\frac{1}{r}\frac{\partial}{\partial r}\left(\mu r\frac{\partial V_\varphi}{\partial r}\right)+\frac{\partial}{\partial z}\left(\mu r\frac{\partial V_\varphi}{\partial z}\right)-\frac{V_\varphi}{r^2}\frac{\partial}{\partial r}(\mu r)\right) \tag{3}$$

$$\frac{1}{A}\frac{\partial(\rho V_z)}{\partial\tau}+\frac{1}{r}\frac{\partial}{\partial r}(\rho r V_r V_z)+\frac{\partial}{\partial z}(\rho V_z V_z)$$
$$=-\frac{\partial p}{\partial z}+E_3\left(\frac{1}{r}\frac{\partial}{\partial r}\left(\mu r\left(\frac{\partial V_z}{\partial r}+\frac{\partial V_r}{\partial z}\right)\right)+\frac{\partial}{\partial z}\left(2\mu\frac{\partial V_z}{\partial z}\right)\right)-\frac{\rho}{Fr} \tag{4}$$

in the above, $\rho=\alpha\rho_1+\beta\rho_2+\gamma$, $\mu=\alpha\rho_1\nu_1+\beta\rho_2\nu_2+\gamma$, which are

$$\alpha=\begin{cases}1, & r\in\text{lower layer},\\ 0, & r\in\text{upper layer};\end{cases}$$

$$\beta=\begin{cases}1, & r\in\text{middle layer},\\ 0, & r\in\text{lower or upper layer};\end{cases}$$

$$\gamma=\begin{cases}1, & r\in\text{upper layer},\\ 0, & r\in\text{lower layer};\end{cases}$$

Also, in the above equations, (V_r, V_φ, V_z), ρ and p denote respectively the dimensionless velocities, density and pressure. In the nondimensionalization, the scales for velocity, length, time, density and pressure are respectively $u^*(\equiv\Omega R)$, H, $1/\Omega$, ρ_3^* and $\rho_3^* u^{*2}$.

In the formulation, it is apparent that the relevant nondimensional parameters are the Ekman number, $E=\frac{\nu^*}{\Omega R^2}$; Froude number, $Fr=\frac{(\Omega R)^2}{gH}$; density ratios, $\rho_1=\rho_1^*/\rho_3^*$, $\rho_2=\rho_2^*/\rho_3^*$; kinematic viscosity ratios, $\nu_1=\nu_1^*/\nu_3^*$, $\nu_2=\nu_2^*/\nu_3^*$; aspect ratio, $A=R/H$.

The associated boundary conditions are:

$V_r=0$ at $r=R/H$, $z=0, 1$;

$V_z=0$ at $r=R/H$, $z=0, 1$;

$V_\varphi=1$ at R/H;

$V_\varphi=r$ at $z=0, 1$

$V_\varphi=0$, $\frac{\partial V_z}{\partial r}=\frac{\partial V_r}{\partial r}=0$ as $r\to 0$.

The relevant parameters for actual computations were set in conformity with the earlier two-layer spin-up problem of Kim & Hyun (1994):

$$A=R/H=0.22,\ Fr=0.4215$$
$$\rho_1=0.5573,\ \rho_2=0.7456$$

In an effort to depict the qualitative character of low, five sets of kinematic viscosity ratios are considered :

Set 1 : $\nu_1=0.01,\ \nu_2=0.1$
$(E_1=1.33\cdot10^{-4},\ E_2=1.33\cdot10^{-3},\ E_3=1.33\cdot10^{-2})$.

Set 2 : $\nu_1=100.0,\ \nu_2=10.0$
$(E_1=1.33\cdot10^{-1},\ E_2=1.33\cdot10^{-2},\ E_3=1.33\cdot10^{-3})$.

Set 3 : $\nu_1=1.0,\ \nu_2=0.1$
$(E_1=1.33\cdot10^{-2},\ E_2=1.33\cdot10^{-3},\ E_3=1.33\cdot10^{-2})$.

Set 4 : $\nu_1=1.0,\ \nu_2=10.0$
$(E_1=1.33\cdot10^{-3},\ E_2=1.33\cdot10^{-2},\ E_3=1.33\cdot10^{-3})$.

Set 5 : $\nu_1=1.0,\ \nu_2=1.0$
$(E_1=1.33\cdot10^{-2},\ E_2=1.33\cdot10^{-2},\ E_3=1.33\cdot10^{-2})$.

Evidently, these parameters sets are selected to exemplify respectively the flow configurations for $\nu_3>\nu_2>\nu_1$, $\nu_3<\nu_2<\nu_1$, $\nu_3=\nu_1>\nu_2$, $\nu_3=\nu_1<\nu_2$ and $\nu_3=\nu_2=\nu_1$.

In numerical computations, a control-volume approach is adopted to discretize the nonlinear, coupled-system of partial differential equations. These discrete equations form a set of coupled algebraic equations, which are solved iteratively by the SIMPLER method (Patankar, 1980). The governing equations are solved on the axisymmetric grid in the $(r\text{-}z)$ plane. All the variables represent the cell-centered quantities, and the velocity components are defined on the cell faces.

The numerical tool to capture the defomation of interfaces follows closely the Height of Liquid method, which was developed by Nichols & Hirt (1971). The reliability and accuracy of the present numerical methodology was validated by repeating the established test problems. Examples include the nonequilibrium rod (Brackbill et al., 1992) and the two-layer liquid in a rotating cylinder (Lim et al., 1993 ; Kim and Hyun, 1994). The numerical results demonstrated broad agreement with the previously-published results in the literature.

The number of grid points was tested in sufficient detail, and, for most computations, a (100×240) mesh in the $(r\text{-}z)$ plane, with time step $\Delta\tau=10^{-3}$, was utilized. A further reduction in the step sizes leads to no noticeable change in the computed output.

3. Results and Discussion

The evolution of meridional flow, together with the deformation of interfaces in the $(r\text{-}z)$ plane, is exemplified in Fig. 2 for Set 1. Within each layer, the meridional stream function ψ is defined such that $\rho V_r=\frac{1}{r}\frac{\partial\psi}{\partial z}$ and $\rho V_z=-\frac{1}{r}\frac{\partial\psi}{\partial r}$. Here, the fluid is incompressible, and ρ denotes the local value within the pertinent layer. Therefore, the lines of equivalues of ψ within each layer indicates the lines of equal values of mass flow rate in the meridional flow field. At small times after the start, both of the interfaces rise at small radii near the central axis and descend at large radii near the sidewall. The kinematic viscosity in the upper layer is smaller than in the lower layer ; therefore, the lower layer attains a faster degree of spin-up, approaching the solid-body rotation in a shorter period of time. At intermediate times, the interfaces gradually sink at small radii and rise near the periphery. At large times, the entire fluid system approaches the rigid-body rotation and the interfaces tend to the characteristic paraboloid shape, with the concave-surface upward with a minimum at the axis. At small times, the meridional flows are intense near the bottom endwall disk and around the interfaces. In the intermediate stages, since the upper and middle layers have gained considerable angular velocities, the meridional flows in these regions weaken accordingly. At large times, the meridional flows subside in general, as expected.

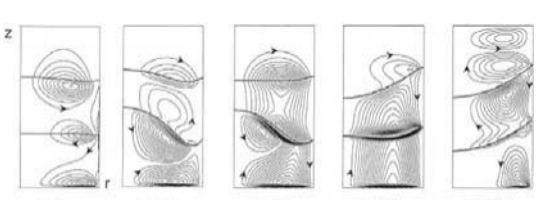

Fig. 2 Plots describing the meridional flow field for Set 1. Values of ψ are normalized by $E_3^{1/2}\Omega R^3$

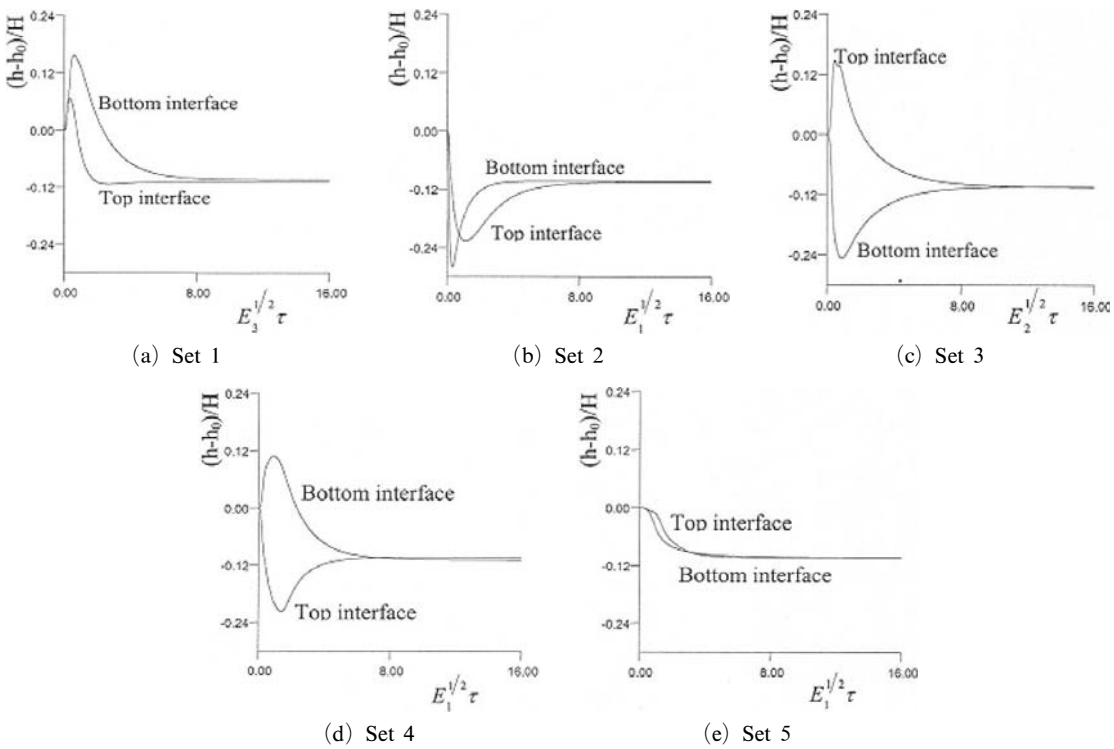

Fig. 3 Time history of the interface displacement at the axis

The time-dependent deformations of interfaces, observed at the axis, are illustrated in Fig. 3(a) for Set 1. As is apparent in the figure, the deformation of the bottom interface is more notable than of the top interface. As can be inferred, since $E_1 < E_3$, the top interface reaches the final state faster than the bottom interface.

The results for Set 2, which represents the opposite case ($\nu_1 > \nu_2 > \nu_3$), is of interest. As displayed in Fig. 4 and Fig. 3(b), the interfaces sink (rise) in the center (periphery) region at small and moderate times. This reflects the development of a low (high) pressure region in the central (periphery) zone. At intermediate times, the levels of the interfaces at the axis reach minimum values. This indicates that the difference in azimuthal velocities in these layers is large. Afterward, the interfaces gradually approach the final-state paraboloid. Since $E_1 > E_3$, the bottom interface reaches the steady state faster than the top interface.

The results for Set 3, for which $\nu_1 = \nu_3 > \nu_2$ are exhibited in Fig. 5. The kinematic viscosity in

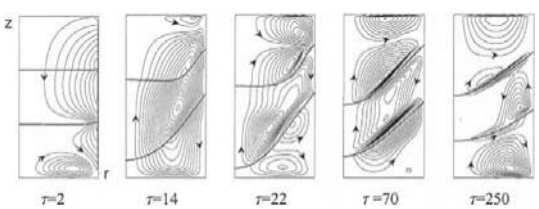

Fig. 4 Plots describing the meridional flow field for Set 2. Values of ψ are normalized by $E_1^{1/2}\Omega R^3$

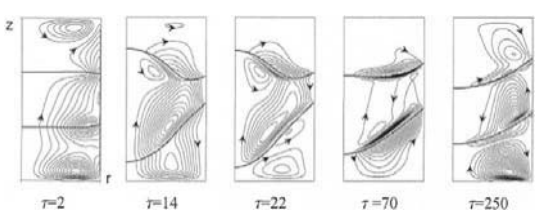

Fig. 5 Plots describing the meridional flow field for Set 3. Values of ψ are normalized by $E_2^{1/2}\Omega R^3$

the middle layer is the smallest, which indicates that the middle layer is spun-up latest. Therefore, at small times, the top (bottom) interface rises (sinks) at the central axis region. In this case, around $\tau \sim 22$, the level of the top (bottom) in-

terface at the axis reaches a maximum (minimum). Afterward, the shapes of interfaces gradually tend to the final- state paraboloids, and the meridional flows subside accordingly.

It should be remarked that, in the present study, the final-state represents a rigid-body rotation, and no internal flows exist. The Sweet-Eddington flow, which occurs in density-stratified fluids, is ignored in the present formulation by limiting to a range of small Froude numbers (Greenspan, 1968 ; Flor et al., 2002).

Results for Set 4 ($\nu_1=\nu_3<\nu_2$) are shown in Fig. 6. The spin-up is fastest in the middle layer. At small times, the pressure in the central axis region in the middle layer is lower than in the periphery region. Consequently, at small times, the top (bottom) interface sinks (rises) in the axis region. At intermediate and large times, the upper and lower layers approach the final-state at approximately equal times.

Figure 7 illuminates the case when the kinematic viscosities in all layers are equal. At small times, spin-up proceeds at nearly equal speeds in the three layers. Therefore, the pressure is lower in the axis region than in the periphery ; both of

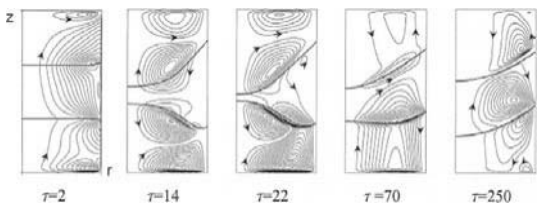

Fig. 6 Plots describing the meridional flow field for Set 4. Values of ψ are normalized by $E_1^{1/2}\Omega R^3$

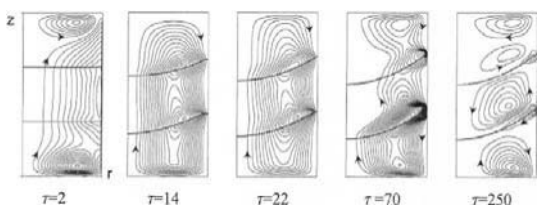

Fig. 7 Plots describing the meridional flow field for Set 5. Values of ψ are normalized by $E_1^{1/2}\Omega R^3$

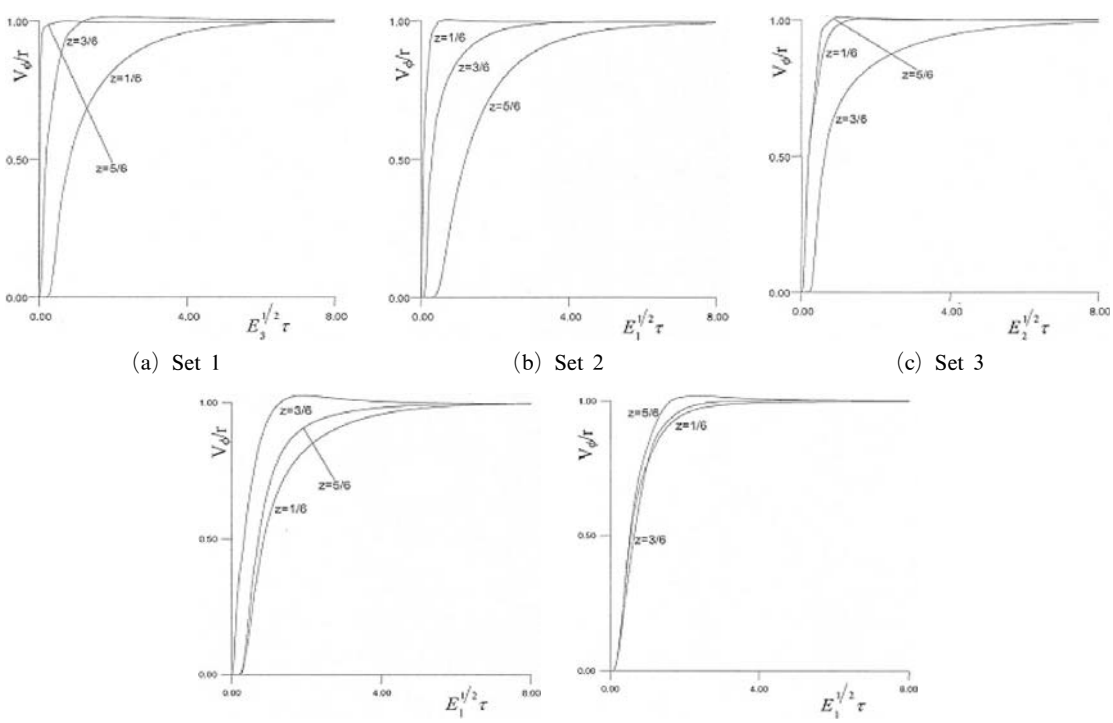

(a) Set 1 (b) Set 2 (c) Set 3

(d) Set 4 (e) Set 5

Fig. 8 Time history of the angular velocity, V_ϕ/r. The position is at $r=1/2$ and $z=1/6$, 3/6, 5/6

the interfaces sink (rise) in the axis (periphery) region. Also, $\rho_3^* > \rho_2^* > \rho_1^*$, the fluid motions are most (least) intensified in the lower (upper) layer. The approach to the final-state is fastest in the lower region.

Summarizing the computed results, the time history of angular velocity, V_ϕ/r, is exhibited in Fig. 8. The locations are at $r=1/2$, and $z=1/6$, $3/6$ and $5/6$, which represents the points in the lower, middle and upper layer. Clearly, the overall spin-up is characterized by the spin-up time scale $\mathbf{E}^{-1/2}$ (or $\mathbf{Re}^{1/2}$). The speed of spin-up in each layer is determined by the value of Ekman layer in each layer. These observations are in line with the general understanding of the spin-up dynamics.

It should be remarked here that some values of E used in the computations, such as $E \sim 10^{-1}$, may not be sufficiently small. In these cases, diffusion from the sidewall and endwall may not be insubstantial, and the present procedures need to be modified. For the bulk of computations, however, the ranges of E values are small enough to sustain the qualitative validity of the present results.

4. Conclusions

The deformation of the interface and the associated fluid motion are vigorous at small times. When the kinematic viscosity is smaller in the upper layer than in the middle layer, the top interface rises (sinks) in the central axis (periphery) region. When the kinematic viscosity is smaller in the lower layer than in the middle layer, the bottom interface rises (sinks) in the periphery (central axis) region. At large times, as spin-up proceeds, the shapes of the interfaces tend to the paraboloids. Systematic experimental verifications of the present results are defined. This could lead to an extension to a multi-layer fluid system.

References

Baker, G. R. and Israeli, M., 1981, "Spin-Up from Rest of Immiscible Fluids," *Studies in Applied Mathematics*, Vol. 65, pp. 249～268.

Brackbill, J., Kothe, D. B. and Zemach, C., 1992, "A Continuum Method for Modeling Surface Tension," *J. Comput. Phys*., 100, pp. 335～354.

Flor, J. B., Ungarish, M. and Bush, J. W. M., 2002, "Spin-up from Rest in a Stratified Fluid : Boundary Flows," *Journal of Fluid Mechanics*, 472, pp. 51～82.

Greenspan, H. P. and Howard, L. N., 1963, "On a Time Dependent Motion of a Rotating Fluid," *Journal of Fluid Mechanics*, Vol. 17, Part 3, pp. 385～404.

Greenspan, H. P., 1968, "The Theory of Rotating Fluids," *Cambridge, UK : Cambridge Univ. Press*., 327 pp.

Kim, K. Y. and Hyun, J. M., 1994, "Spin-up From Rest of a Two-layer Liquid in a Cylinder," *J. of Fluid Engineering*, 116, pp. 808～814.

Lim, T. G., Choi, S. and Hyun, J. M., 1993, "Transient Interface Shape of a Two-layer Liquid in an Abruptly Rotating Cylinder," *J. of Fluid Engineering*, 115, pp. 324～329.

Nichols B. D. and Hirt C. W., 1971, "Calculating Three-Dimensional Free Surface Flows in the Vicinity of Submerged and Exposed Structures," *J. Comp. Phys*., 12, 234.

Patankar S. V., 1980, "Numerical Heat Transfer and Fluid Flow," Hemisphere, Washington, DC.

Wedemeyer, E. H., 1964, "The Unsteady Flow within a Spinning Cylinder," *Journal of Fluid Mechanics*, Vol. 20, Part 3, pp. 383～399.

Weidman, P. D., 1976, "On the Spin-Up and Spin-Down of a Rotating Fluid. Part I : Extending the Wedemeyer Model. Part II : Measurements and Stability," *Journal of Fluid Mechanics*, Vol. 77, Part 4, pp. 685～735.